SHEAR AND ANCHORAGE FAILURE OF SCALE PRESTRESSED CONCRETE I-GIRDERS AND SCALE BRIDGE SECTION

Cameron D. Murray
University of Arkansas
Department of Civil Engineering
4183 Bell Engineering Center
Fayetteville, AR 72701
USA

Royce W. Floyd
The University of Oklahoma
School of Civil Engineering & Environmental Science
202 W. Boyd St., Room 334
Norman, OK 73019
USA

KEYWORDS: Prestressed concrete, bridges, shear, anchorage, bond

ABSTRACT

A series of scale (572 mm deep) prestressed concrete I-girder sections were constructed to investigate shear behavior when loaded at the quarter span point. An accompanying scale bridge (5.5 m long and 4.1 m wide) was constructed out of the same sections to observe system level behavior and compare to the individual sections. All failures were controlled by anchorage of the prestressing strands; however, observations were made about the post-girder failure behavior of the bridge section. Failure mechanisms were the same in the individual sections as in the scale bridge, but the scale bridge maintained structural integrity at much larger loads and the deck and full-depth diaphragms provided a means of load redistribution after the loaded girder failed. A punching shear failure in the deck brought the test to a close, however damage indicative of two-way slab behavior was observed in the deck. This suggests different failure behavior than is typically assumed for a bridge deck. Qualitative information about the tests is shared along with pictures detailing the observed failure modes. The full-depth diaphragms were observed to have an important influence on the failure of the bridge and this result warrants further consideration.

INTRODUCTION

Figure 1: Two full-scale girders being delivered for testing, Girder A (top) and Girder C (bottom)

Prestressed concrete girder bridges are frequently used on interstate highways in the United States (U.S.). As of 2016, approximately 25% of all U.S. bridges were prestressed concrete (Federal Highway Administration 2016). In the state of Oklahoma there were 4,582 prestressed concrete bridges in service in 2016. Many of these bridges were built in the early days of the interstate highway system and are

approaching 40 years in service. Since many of these bridges are simply supported with expansion joints at the supports, corrosion of the prestressing strands is very common. There was concern on the part of the Oklahoma Department of Transportation around 2013 that this corrosion may affect the anchorage of the prestressing strands and ultimately the shear capacity. The following paper details part of a study performed by the authors to investigate the shear and anchorage behavior in prestressed concrete girder bridges. The complete study can be found in other works by the authors (Murray 2017) (Floyd, et al. 2016). In the full study, two decommissioned prestressed concrete girders with corrosion damage (Figure 1) were loaded close to the ends to investigate their shear capacity. The full scale girders were called Girders A and C. These tests were accompanied by tests of scaled prestressed concrete girders and the testing of a scale bridge section. This paper will describe the scale girder tests and how they compared to the scale bridge test in terms of their failure mechanisms.

BACKGROUND

Shear capacity of prestressed concrete sections can be complicated to predict. The typical assumption of a linear strain distribution may not be accurate in regions close to the supports, where shear forces are the highest (Darwin, Dolan and Nilson 2016). The additional strains from the prestress force is a further complication. Another issue that can arise when prestressed concrete members crack in shear is a loss of bond of the prestressing strands. When shear cracks close to the end of a prestressed concrete member interrupt the transfer or development length of the strands a loss of anchorage can reduce the shear capacity since the prestress force typically directly resists the tension stressed due to shear. Corrosion of the prestressing strands can induce cracking towards the ends as well, increasing the likelihood of bond loss. Finally, another confounding factor related to bridges is the connectivity of several girders through the concrete deck and end and intermediate diaphragms (Figure 2). For these reasons it can be complex to estimate the shear capacity of a prestressed concrete section accurately.

Figure 2: View from underneath scale bridge showing connection between girders and slab and the end diaphragm connection

In the U.S. several methods exist to calculate shear capacity of prestressed concrete. The American Concrete Institute's Building Code Requirements for Structural Concrete (ACI 318) (American Concrete Institute 2014) uses a partially empirical process to determine the shear strength of a member. For bridges, the American Association of State Highway and Transportation Officials (AASHTO) Load and Resistance Factor Design (LRFD) Bridge Design Specifications (AASHTO 2015) contains multiple options to calculate shear strength. The traditional methods are somewhat similar to the ACI methodology, on the other hand AASHTO also provides a method utilizing Modified Compression Field Theory, a method that takes into account the assumed strain distribution in the web of concrete members.

All of the current methods have limitations. These methods cannot account for reduced bond capability of the strands or for any additional resistance provided by the bridge deck or secondary elements in the bridge such as diaphragms. While the current methods may occasionally predict the strength of individual prestressed concrete girders with accuracy, the system level behavior is only accounted for by sharing the total demand between girders using load distribution factors. In this paper, the qualitative response of individual scale girders tested close to the ends is compared to the response of a scale bridge to observe effects of system behavior on shear capacity and behavior.

DESCRIPTION OF SPECIMENS

All of the specimens used in this study were constructed in the Donald G. Fears Structural Engineering Laboratory at the University of Oklahoma (OU). The scale girders used were meant to be roughly half scale replicas of standard AASHTO type-II girders (Dimensions shown in Figure 3). More details about the complete design of the scale girders can be found in the previously cited documents by the authors (Murray 2017) (Floyd, et al. 2016). In short, the prestressed and mild steel reinforcement were designed to be similar to the full-scale girders tested by the authors. This was meant to provide a realistic proportion of shear steel for the girders and to try to roughly match the service stress levels of the full-scale girders in the half-scale replicas.

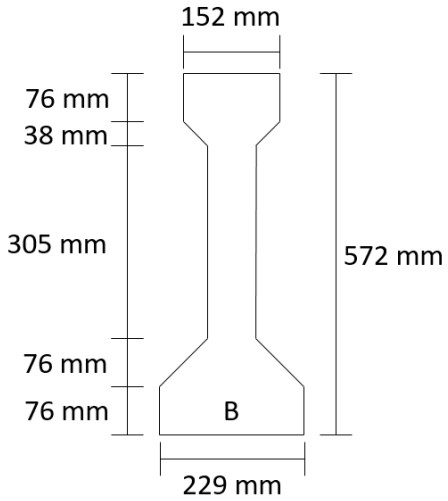

Figure 3: Dimensions of scale girders

Four half scale sections were constructed based on design details from the two full-scale girders (Girders A and C). These sections had slightly different applied prestress forces but were otherwise very similar in design. The concrete for these girders was made in Fears lab and all prestressing was performed by members of the research team on the prestressing bed at OU (Figure 4). Each girder was 5.5 m long.

Figure 4: Scale girder shear steel and prestressing strands (left) and completed girder prior to de-tensioning (right)

Once the scale girders were cast, an additional 108 mm thick deck section was cast separately atop the girders to match the dimensions of the remaining deck in the full-scale sections. Figure 5 shows the completed girder sections at different stages of deck casting. Figure 5a shows the sections with a wider portion of deck, to match the full scale Girder C dimensions, while Figure 5b shows the smaller deck (Girder A). The four individual scale sections were then tested using a single point load at varying distances form the support.

Figure 5: Completed scale girder specimens with sections of deck prior to and after casting

Figure 6: Scale bridge construction progress

Another four scale girders were cast using the same techniques to construct a scale bridge. The scale bridge was simply supported on neoprene bearing pads and consisted of four girders connected by a deck and middle and end diaphragms cast monolithically with the deck. Figure 6 shows the construction

steps for the scale bridge. It was constructed in much the same way as a real prestressed concrete bridge. The girders were arranged and formwork for the deck and diaphragms was constructed onto the girders. The concrete for the deck and diaphragms was poured, allowing the girders to carry the full dead load of the deck and diaphragms. The bottom right of Figure 6 shows the completed bridge with a special made load frame located at the quarter span point of the bridge. Several sets of tests were performed along the width of the bridge at the quarter span point to evaluate computer models of the scale bridge. Next the bridge was loaded to failure by increasing a point load located above an interior girder at the quarter span point. This location was selected to maximize shear demand in a region likely characterized by beam-type shear (not a discontinuity region) and to compare more readily with the scale individual girder tests and the full-scale tests.

The completed scale bridge was 5.5 m long, 4.1 m wide and the deck was 108 mm deep. An array of sensors was set up around the scale bridge to measure strains, deflections, strand slip, and applied load. For this paper the qualitative behavior of the individual girders and scale bridge as well as the ultimate loads will be discussed. More information about the tests can be found in the reports cited in this document as well as in forthcoming journal papers by the authors.

TEST RESULTS

A summary of the individual girder test results is given in Table 1. All tests consisted of a single point load. The load location is given from the end of the girder closest to the load point. *a/d* refers to the shear span to depth ratio. Some values are given for the ultimate load supported, the maximum shear force, and the maximum moment. All failures appeared to be bond-related. This section will describe the individual girder failures followed by how they compare to the scale bridge test. Note the naming convention in Table 1, A1 and A2 are two girders that were designed based on the first full-scale girder tested (Girder A) and C1 and C2 are two girders designed to mimic the reinforcement of the second full-scale girder tested (Girder C). Again, the only difference between these two was the service stress state.

Table 1: Summary of scale girder tests

Property/Result	**A1s**	**A2s**	**C1s**	**C2s**
a/d	2.4	3.0	3.0	2.4
Load Location (m)	1.37	1.82	1.82	1.37
P_{max} *(kN)*	208	199	277	189
V_{max} *(kN)*	161	138	190	148
M_{max} *(kN-m)*	206	240	330	190
Failure Mode	Bond-Shear/Flexure	Bond-Shear	Bond-Shear	Bond-shear

The final behavior of girder A1s is shown in Figure 7. Extensive shear and flexural cracking was observed, and there was some ductility after initial cracking and strand slip. Crushing in the deck occurred at the final load increments. By the end of the test, a maximum slip of 16.3 and 16.8 mm was measured for the strands at the loaded end. The maximum point load for flexure at this location was 209 kN based on strain compatibility compared to a maximum load in the test of 208 kN. This is a difference of about 1.7 percent. This was very close to the actual load despite significant bond loss, potentially indicating that some yielding occurred. While the anticipated failure was flexural, shear cracking occurred near the end and led to strand slip. It became impossible to apply additional load to the girder once slip occurred. For test A1s and C2s the load was placed at an a/d ratio of 2.4, corresponding to the quarter span point of the girder. This location was chosen because in older bridge specifications this location was taken as the critical section for shear demand. Because in test A1s the failure was controlled by bond, the load was moved further form the support for test A2s.

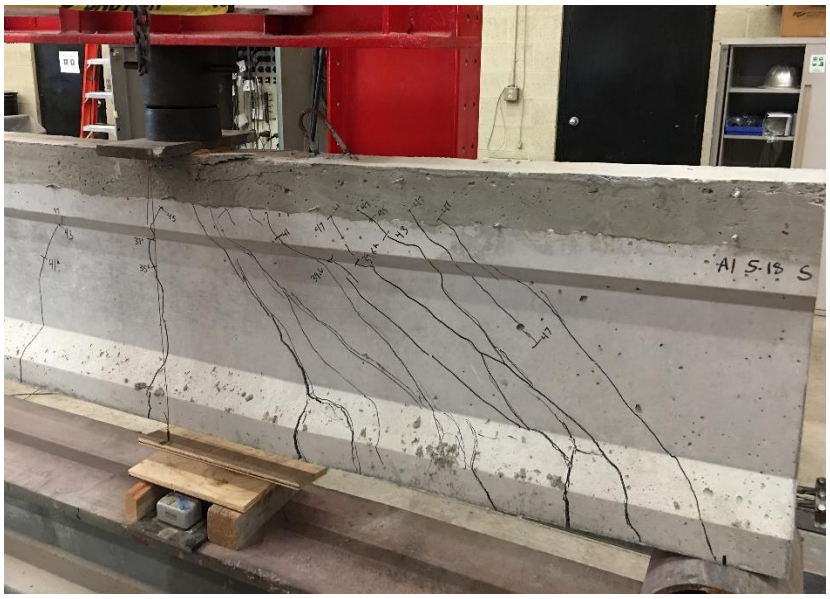

Figure 7: Girder A1s failure

The final cracking of girder A2s is shown in

Figure 8. Extensive shear and flexural cracking was observed, and there was limited ductility after initial cracking. The strand slip and shear cracking at 199 kN reduced the load carrying ability of the girder. Crushing in the deck was not observed but some shear cracks oriented themselves horizontally near the top of the deck. By the end of the test, a maximum slip of 15.0 and 15.5 mm was measured for the strands at the loaded end. The maximum point load for flexure at this location was 187 kN based on strain compatibility compared to a maximum load in the test of 199 kN kips. This is a difference of 6.7 percent. Again, this was good agreement despite bond failure, indicating that slip potentially occurred after some strand yielding occurred. Again ultimate load was limited based on slip in the strands despite locating the load further into the section.

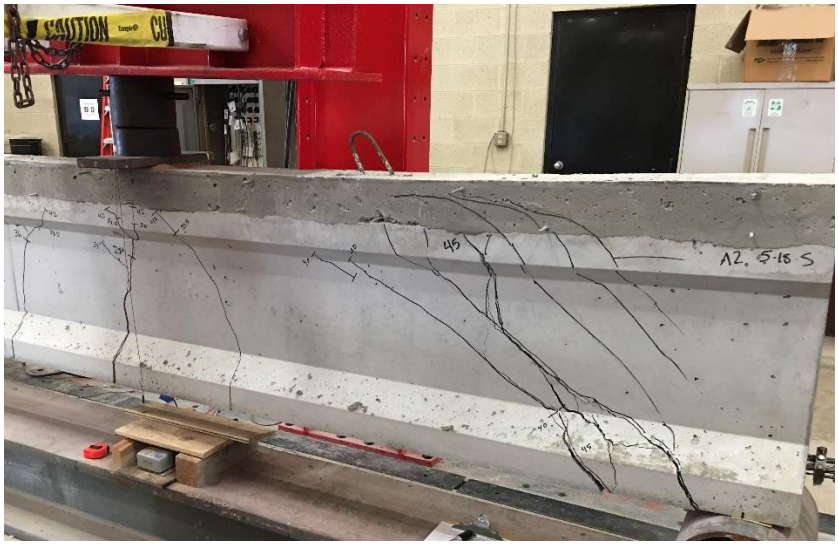

Figure 8: Girder A2s failure

Test C1s was performed at an *a/d* ratio of 3.0, corresponding to the *a/d* ratio of full-scale girder test C1. This *a/d* ratio resulted in a load point located at a distance of 1.82 m from the end of the girder. Initially the girder was quite stiff, with only 3.3 mm of deflection when the first flexural cracking occurred at a load of 185 kN. After initial flexural cracking, load was increased at 2 kip increments. At a load of 205 kN, shear cracks formed near the supports. The formation of these shear cracks led to strand slip of 0.51

mm for one strand on the south end of the girder. Slip increased from the point of shear cracking to the end of the test, resulting in a maximum slip of 13.2 and 18.3 mm for the strands on the loaded end. The test was continued to a maximum applied force of 277 kN, at which point the strand slip prevented any increase in load. The flexural capacity based on strain compatibility at this section corresponded to a point load of 240 kN. The shear capacity using the ACI method at this section corresponded to a point load of 329 kips. The predicted capacity was exceeded for flexure despite the large amount of recorded slip. The partial center diaphragm appeared to arrest cracking near midspan, but it is difficult to make definite conclusions on the effect of the partial diaphragms since the tests of scaled girders without diaphragms were for a slightly different design (smaller prestress force).

Figure 9: Girder C1s failure

Test C2s was performed at an a/d ratio of 2.4, corresponding to the quarter-point of the girder. This location was chosen since this is the location where the scale bridge would be tested and was the location of full-scale test C2. The load point was located at a distance of 1.37 m from the end of the girder for this configuration. As with test C1s, little deflection was measured before cracking. A large shear crack formed at the support at a load of 180 kN and 2.29 mm of deflection. When this shear crack formed, slip of 0.79 and 0.94 mm was observed for the strands on the loaded end. Because of the proximity of the initial shear cracks to the support, slip increased with applied load after cracking, which prevented any increase in load. The maximum load reached in this test was 189 kN and the test was stopped when some crushing was observed in the deck. The maximum deflection was 46.4 mm The cracking pattern from this test is shown in Figure 10. Loss of bond between the prestressing strands and the concrete prevented the girder from reaching its estimated capacity. The girder's nominal moment capacity corresponded to a point load based on strain compatibility of 288 kN. The shear capacity by the ACI method corresponded to a point load of 365 kN. The capacity of the girder was reduced due to strand slip that began with initial shear cracking.

Figure 10: Girder C2s failure

Unfortunately, the slip in every test was a limitation of the dimensions of the test specimens. Since the development length of the strands used for these specimens is roughly 2.3 mm, the short embedment length required for this test influenced the bond behavior. Additionally, it is possible the stiffness of the end diaphragm may have influenced the test. The initial cracking occurred in shear at a very low deflection. It is possible the diaphragm contributed to the stiffness of the end region. Tests of girders A1s and A2s helped to evaluate the influence of the diaphragms on girder behavior, but again were for a slightly different girder design which reduces the applicability of the comparison. Another possibility is that the increased stiffness due to the available deck influenced the shear behavior.

The scale bridge was composed of the girder A half-scale designs. Load was placed at the quarter span point of an interior girder for the destructive test of the bridge (a/d = 2.4). Initial web shear cracking in the girder was observed at a load of 245 kN. The initial observed crack is marked on this figure and the location where slope changed is also marked. The initial web shear crack occurred at a load 191 kN and is shown in Figure 11.

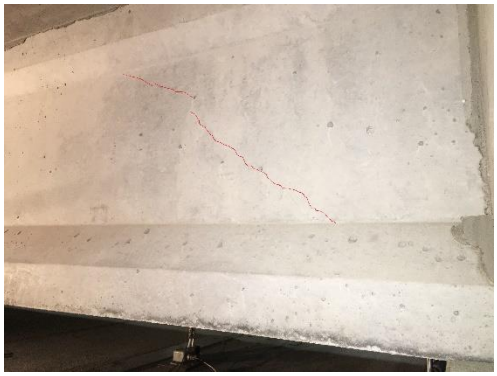

Figure 11: Initial crack during scale bridge test

Shear cracks extended into the bottom flange at a load of 254 kN, and a flexural crack was observed beneath the load point at a load of 280 kN. It is very likely that this crack appeared before this load, but direct observation was difficult due to the crack's interior location. At this load, there was approximately 0.51 mm of slip in the strands of the loaded girder. It is possible that the apparent slip measurements were affected by shifting concrete at the end when the diaphragms cracked and separated from the girders. At a load of 298 kN, another shear crack appeared roughly 0.61 m into the span from the previous crack. Between 298 and 334 kN of load, a bond-shear type crack appeared on the loaded girder and a diagonal crack indicative of two-way slab bending behavior appeared in the deck (Figure 12). The slab crack extended from the southeast corner of the bridge where the diaphragm and slab meet to the load point. At a load of 347 kN, cracking in the exterior girder occurred where the diaphragm connected to the girder. Load was applied up to a maximum of 429 kN, When the load point punched through the bridge deck. This was accompanied by extensive cracking in the loaded girder.

Figure 12: Bond shear cracking in loaded girder (left) and two way type cracking in deck slab (right)

The final state of the bridge is shown from above in Figure 13. The cracking is indicative of two-way slab bending. The cracks form a roughly circular pattern about the load point terminating at the middle diaphragm and adjacent girders. The cracking at the end diaphragm is different, likely because there is less stiffness – the diaphragm rotated away from the bridge during the test resulting in less fixity at the end of the slab. This two-way behavior implies greater load resistance than the one way bending typically assumed for a bridge deck in this configuration. This may explain the much larger resistance found in the bridge compared to the individual girders tested.

Figure 13: Cracking in scale bridge deck after testing

Figure 14 shows the punching shear failure in the bridge deck. The loaded girder in the scale bridge experienced a failure that was very similar (Figure 15) to the individual scale section A1s (tested at the same a/d ratio). Cracking and slip was observed at a higher load for the bridge section than for the individual section. Cracking occurred at a load of 151 kN in A1s, but at 191 kN in the bridge test. Slip was observed at a load of 169 kN in A1s and 222 kN in the bridge test. The ultimate capacity was also increased 102%, from 213 kN in the individual section, to 429 kN in the bridge deck. This is a significant increase, particularly when the predicted ultimate loads for the two cases were 209 kN for A1s and 222 kN for the bridge (assuming a tributary width equal to the girder spacing). The girder had much larger post cracking and post slip stiffness due to the transfer of load through the diaphragm and the slab to the adjacent girders. Based on the results of the scale bridge test, the diaphragms and their connections to the girders provides additional load distribution after a loaded girder fails.

Figure 14: Punching shear failure in deck

Figure 15: Final cracking in loaded bridge girder

Apparently the bridge deck and diaphragms provide an important means of load transfer post-girder failure. This load transfer is not accounted for in bridge design where the girder capacities are taken individually. This seems to imply that end and intermediate diaphragms should be detailed in bridges for their load transfer capabilities as an extra means of redundancy. If the deck were allowed to bend as a one-way slab, without the connection to the diaphragms, the capacity of the bridge may have been reduced.

CONCLUSIONS

While the general failure mechanisms in the scale individual sections and the scale bridge were similar (bond and shear failure), the capacities differed. In the scale bridge there was additional capacity after the girder cracked extensively and slip was measured which can be attributed to the two-way bending of the deck. This two-way bending was only possible due to the full-depth diaphragms at the ends and middle of the bridge deck. The two-way bending was apparent due to diagonal cracks on the underside of the deck and a circular crack pattern around the load point. The bridge ultimately failed due to punching shear, it is possible more load could have been carried if the load were more spread out as in a real bridge. Girder tests can only tell us so much about the shear capacity of bridges because the full bridge section allows redistribution of forces as a girder fails, especially if end and middle diaphragms are provided. If diaphragms were not present it is possible the bridge would have failed sooner.

REFERENCES

AASHTO. 2015. *AASHTO LRFD Bridge Design Specifications.* Washington, D.C.: American Association of State Highway and Transportation Officials.

American Concrete Institute. 2014. *ACI 318: Building Code Requirements for Structural Concrete.* Farmington Hills, MI: ACI.

Darwin, D, C.W. Dolan, and A.H. Nilson. 2016. *Design of Concrete Structures.* 15th. New York, NY: McGraw Hill Education.

Federal Highway Administration. 2016. "National Bridge Inventory." February 19. https://www.fhwa.dot.gov/bridge/nbi.cfm.

Floyd, Royce W., Jin-Song Pei, Cameron D. Murray, Brittany Cranor, and Peng Tang. 2016. *Understanding the behavior of prestressed girders after years of service.* Oklahoma City, OK: Oklahoma Department of Transportation.

Murray, Cameron D. 2017. *Understanding Ultimate Shear Behavior of Prestressed Concrete Girder Bridges as a System Through Experimental Testing and Analytical Methods.* Norman, OK: The University of Oklahoma.